



Curcumin Loaded Fe_3O_4 Nanoparticles: An MRI Contrast Agent to Investigate the Impact of Curcumin on Maximizing Negative Contrast and r_2 Relaxation Rate

Milad Ghorbaanee¹ · Amir Ahmad Salarian¹ · Valiollah Saba²

Received: 20 March 2018 / Accepted: 28 April 2018 / Published online: 2 May 2018
© Springer Science+Business Media, LLC, part of Springer Nature 2018

Abstract

The goal of this project was to fabricate a diagnostic system based on polyethylenimine (PEI) coated superparamagnetic iron oxide nanoparticles (Fe_3O_4 NPs) containing curcumin (CUR) in order to appraise the influence of CUR on increase of r_2 relaxation rate of a negative contrast agent in magnetic resonance imaging (MRI). Based on the obtained results, the structural properties of the final product (i.e., Fe_3O_4 -PEI-CUR NPs) were validated according to the initial hypothesis (i.e., NPs of about 50 nm in diameter with proper magnetic properties). Also, the CUR to Fe_3O_4 -PEI NPs weight ratio of 2:1 was determined as an optimal ratio resulting in an 8% increase in the amount of loaded CUR as compared to the weight ratio of 1:1. In addition, CUR release from Fe_3O_4 -PEI-CUR NPs was evaluated at two pH of 5.5 and 7.4 which revealed that the CUR release mechanism was pH-sensitive. The visual and numerical data of in vitro MRI all suggested an increase in negative contrast in the presence of CUR, as the r_2 values for Fe_3O_4 -PEI, Fe_3O_4 -PEI-CUR (30% CUR loading), and Fe_3O_4 -PEI-CUR (38% CUR loading) NPs were determined 78.278, 93.854, and 95.685 (1/mM sec), respectively. It was also shown that an 8% increase of CUR content in Fe_3O_4 -PEI-CUR (38%) NPs merely led to a 2% increase in r_2 and therefore in negative contrast. This result suggested that increasing CUR content more than a specific amount could not improve contrast considerably, while there was a significant difference (about 20%) between r_2 values of Fe_3O_4 -PEI and Fe_3O_4 -PEI-CUR (30%) NPs.

Keywords MRI · Negative contrast agent · SPIONs · Curcumin

1 Introduction

With the prevalence of various diseases, such as cancer, that attack the body's internal and sensitive tissues, a diagnostic method which can accurately capture an image of the body's internal tissues is needed more and more. Meanwhile, the magnetic resonance imaging (MRI) method is known as one of the most common and effective methods for imaging various tissues of the body due to its unique features [1]. The

non-use of ionizing radiation and thus the absence of any harmful effects have made this technique as one of the most significant techniques among the other common diagnostic methods [2]. MRI is a desirable non-invasive imaging method which is commonly used for imaging tumors due to its ability to process cell-level information [3]. In order to increase the accuracy, sensitivity, and consequently the quality of MRI images, contrast agents are applied, which play an important role in increasing the contrast between the healthy and affected tissues [4].

The purpose of this project was to fabricate a diagnostic system, as a negative contrast agent for MRI, based on polyethylenimine (PEI) coated superparamagnetic iron oxide nanoparticles (Fe_3O_4 NPs) containing curcumin (CUR). CUR, as a colorful herbal antioxidant, was utilized to increase the r_2 relaxation rate of the negative contrast agent. In this system, the Fe_3O_4 NPs, as the main core, were responsible for creating a negative contrast (dark signal). Their magnetic property, which makes them steerable in response to permanent external magnetic field, can be used

Electronic supplementary material The online version of this article (<https://doi.org/10.1007/s10904-018-0868-x>) contains supplementary material, which is available to authorized users.

✉ Milad Ghorbaanee
ghorbaaneemilad@yahoo.com

¹ Department of Toxicology, AJA University of Medical Sciences, Tehran, Iran

² Department of Radiology, Faculty of Paramedicine, AJA University of Medical Sciences, Tehran, Iran

for their specific accumulation at a specific part of the body. In recent years, Fe_3O_4 NPs, which are inherently multifunctional, have been studied and used in a wide range of applications, such as drug delivery, magnetic therapy, and MRI [5–10]. This is due to their unique properties including the ability to function at molecular and cellular levels in biological environments [11] and to be functionalized with different materials with the aim of improving their biocompatibility [12].

PEI is a hydrophilic polymer, which has a negligible toxicity in molecular weights of less than 25,000 kDa and can protect NPs from being removed by reticuloendothelial system (RES). Besides, due to the presence of aliphatic groups, it could provide a suitable substrate for loading the CUR and its controlled release. PEI is a cationic polymer that has been widely used for gene delivery [13–15].

CUR, a recognized herbal antioxidant with anti-cancer properties, was used as an agent to intensify the contrast and hence to enhance the quality of the images obtained by the MRI method. The hydrophobic property of CUR was utilized to load it on PEI coated Fe_3O_4 NPs, so that the interaction of CUR with aliphatic groups of PEI led to its adsorption on the polymer. It has been reported that the herbal origin of CUR could reduce its toxicity against healthy tissue cells. For example, based on the results of *in vitro* and *in vivo* studies, Wilken et al. reported that CUR was able to control the proliferation of cancer cells, while its toxicity to healthy cells was far lower [16]. In addition, it has been shown that the color content of CUR could increase the r_2 relaxation rate of the contrast agents containing CUR and, as a result, intensify the contrast in MRI images which could lead to improvement of their quality [17]. This can be also applied to other color-containing compounds, such as Doxorubicin, an anticancer drug [18, 19].

The structural characteristics of the fabricated diagnostic system were evaluated by the standard tests for characterization of nanomaterials, and the ability of CUR to increase r_2 relaxation rate of a negative contrast agent was investigated via *in vitro* MRI.

2 Materials and Methods

2.1 Materials

Ferrous chloride tetra-hydrate ($\text{FeCl}_2 \cdot 4\text{H}_2\text{O}$), ferric chloride hexa-hydrate ($\text{FeCl}_3 \cdot 6\text{H}_2\text{O}$), ammonia solution (NH_4OH , 28%), ethanol (absolute), curcumin (CUR), acetone, acetonitrile, methanol, and hydrochloric acid (HCl) were obtained from Merck (Germany). Polyethyleneimine (PEI) 1300 kD, phosphate buffer saline (PBS) tablets, acetic acid, sodium acetate, triethylamine, and tween-80 were purchased from

Sigma-Aldrich (USA). All materials were used without any further purification.

2.2 Methods

2.2.1 Fabrication of Fe_3O_4 NPs

In order to fabricate Fe_3O_4 NPs, two solutions of $\text{FeCl}_3 \cdot 6\text{H}_2\text{O}$ and $\text{FeCl}_2 \cdot 4\text{H}_2\text{O}$ (with a mole ratio of 2:1) were prepared in deionized water at first [20]. Then, the prepared solutions were well mixed via ultrasonic bath to form a clear solution. Thereafter, the resulted solution was poured into a balloon under mechanical stirrer at 2000 rpm and nitrogen flow. After 10 min, 40 ml of a 28% solution of ammonia (NH_4OH) was added to the solution at once, and the solution's color changed from orange to black. The reaction temperature was adjusted to 60 °C, and after 1 h, a black precipitate was removed by applying an external magnet. The precipitate was washed several times with deionized water and ethanol and dried using a desiccator.

2.2.2 Fabrication of PEI Coated Fe_3O_4 NPs (Fe_3O_4 -PEI)

For this purpose, 200 mg of PEI (1300 kD) and 100 mg of Fe_3O_4 NPs were first mixed well in deionized water under nitrogen flow and vigorous stirring. The solution was then placed under vigorous stirring at 90 °C for 3 h. Finally, the sediment was isolated by applying an external magnet, washed several times with deionized water, and dried in a vacuum oven.

2.2.3 CUR Loading on Fe_3O_4 -PEI NPs (Fe_3O_4 -PEI-CUR NPs)

According to a previously reported method [21] with some minor changes, to load CUR on Fe_3O_4 -PEI NPs with CUR to Fe_3O_4 -PEI weight ratios of 1:1, 2:1, and 3:1, a colloidal solution of Fe_3O_4 -PEI NPs (0.5 mg/ml) was first prepared in deionized water using ultrasonic bath. Then, three solutions of CUR were made in acetone at concentrations of 5, 10, and 15 mg/ml. It is worth noting that the volume ratio of water to acetone was 10:1, so that the combination of two organic and aqueous phases did not lead to aggregation of hydrophilic Fe_3O_4 -PEI NPs, and therefore their specific surface area did not significantly reduce. The colloidal solution of Fe_3O_4 -PEI NPs was then mixed with CUR solutions at the mentioned concentrations. Next, the resulted three solutions were placed in a shaker incubator at 25 °C for 24 h to let the CUR molecules be adsorbed on the surface of Fe_3O_4 -PEI NPs through an electrostatic interaction. After, all three solutions were subjected to an external magnetic field to separate the unconjugated CUR from the environment by separation of CUR loaded Fe_3O_4 -PEI NPs. The process of washing was done and repeated several times via applying

an external magnetic field to ensure that the unconjugated CUR was removed. Supernatants obtained from this process were used to calculate the amount of loaded CUR and kept in refrigerator in dark.

To calculate the amount of CUR loaded on Fe₃O₄-PEI NPs, the CUR calibration curve was first plotted by UV–Vis through recording the absorbance of CUR at 420 nm at different concentrations with water/acetone volume ratio of 10:1. Then, loading content (LC) and the percentage of CUR loaded on Fe₃O₄-PEI NPs (PL) were calculated using the following formulas:

$$LC = \frac{\text{Total CUR(mg)} - \text{free CUR in supernatant (mg)}}{\text{Fe}_3\text{O}_4 - \text{PEI NPs (mg)}} \quad (1)$$

$$PL(\%) = \frac{\text{Loaded CUR (mg)}}{\text{Loaded CUR (mg)} + \text{Fe}_3\text{O}_4 - \text{PEI NPs (mg)}} \times 100 \quad (2)$$

The mean value of triplicate experiments was reported as the final LC and PL of CUR.

2.2.4 In Vitro Evaluation of CUR Release from Fe₃O₄-PEI-CUR NPs

To determine the profile of CUR release from Fe₃O₄-PEI-CUR NPs and investigate its dependence on pH values, 5 mg of the NPs was immersed in 7.5 ml of a phosphate buffer solution (PBS) containing 0.1% w/v Tween-80 at two pH of 5.5 and 7.4. The pH 5.5 represented the intra tumor environment, and the pH 7.4 represented blood plasma environment or normal tissues [22]. It should be noted that the use of tween-80, as a surfactant, was to increase the solubility of the released CUR in the buffer medium. Then, the solutions were placed in a shaker incubator at 100 rpm at 37 °C in a dark environment. At appropriate time intervals (i.e., 0.5, 1, 12, and 24 h) the solutions were centrifuged for 20 min at 11,000×g rpm, and supernatants were extracted from the medium and stored in a dark environment in a refrigerator. After sampling, new buffer solution was added to each container. To calculate the amount of released CUR at each time interval at each pH, CUR calibration curve was first plotted in a similar condition via UV–Vis at 420 nm, and the absorbance of each supernatant was then determined at 420 nm [21]. Absorbance of every supernatant solution was read three times, and the final result was reported through the calculation of the average absorbance.

2.2.5 HPLC Assay

A high-performance liquid chromatography (HPLC) assay was used to assess the presence of CUR in the obtained

supernatant solutions of release process and was done according to a previously reported protocol [23]. Briefly, the mobile phase consisted of acetonitrile, methanol, and acetate buffer solution (20 mM, pH 3) (60:30:10, v/v). To reduce peak tailing, 175 µl of triethylamine was added to methanol (250 ml). The stationary phase consisted of a C18 column with a length of 150 mm and an internal diameter of 4.6 mm [Agilent Technologies 1200 series (USA)]. To run the test, 40 µl of CUR solution in acetonitrile (0.085 mg/ml) was injected into the injection port at the mobile phase flow rate of 0.8 ml/min. The UV–Vis detector wavelength was set to 420 nm to detect CUR. After 2 min of injection, the peak was gradually formed.

The above operation was repeated three times for both samples (i.e., supernatant solutions of release process at pH 5.5 and 7.4) to ensure the accuracy of the assay.

2.2.6 In Vitro MRI Assay

2.2.6.1 Sample Preparation For this purpose, the weight percentage of Fe in the prepared NPs was first determined because the concentration of the samples was calculated based on the concentration of Fe. Therefore, at first, the percentage of Fe was determined 68% in Fe₃O₄-PEI NPs using the ICP-MS analysis. According to this and by knowing the weight percentages of CUR, samples of Fe₃O₄-PEI, Fe₃O₄-PEI-CUR (30%), and Fe₃O₄-PEI-CUR (38%) NPs at concentrations of 0, 0.04, 0.08, 0.16, 0.32, 0.64, and 1.28 (mM Fe) were prepared in PBS (pH 7.4, 2.5% w/v agar solution) according to agar gel phantom method for in vitro MRI assay [21, 23–26].

2.2.6.2 In Vitro MRI In vitro MRI was performed for samples of Fe₃O₄-PEI, Fe₃O₄-PEI-CUR (30%), and Fe₃O₄-PEI-CUR (38%) NPs according to the following procedure and using 1.5 T MRI scanner (Firoozgar Hospital, Tehran, Iran). For T₂ weighted images: TR=2000 (ms), TE=22, 44, 66, 88, 110, 132, 154, 176, 198, 220, 242, 264, 286, 308, 330, and 352 (ms), FOV=200 mm, slice thickness=5 mm, and matrix=192×256. For T₂* weighted images: TR=391 (ms), TE=6.2, 6/4, 6/6, 6/8, 6/10, 6/12, 6/14, and 6/16 (ms), FOV=200 mm, slice thickness=5 mm, and matrix=192×192. T₂ values were calculated using T₂ mapping sequences in the above conditions. The r₂ relaxation rate was also obtained from the gradient of linear fit of 1/T₂ (s⁻¹) versus the Fe concentration (mM).

2.2.7 Characterization

FTIR spectra of the samples were gained by KBr method through a Fourier transform infrared spectrometer (Spectrum Two, Perkin Elmer) in the wavelength range of 500–4000 cm⁻¹. Crystal structure of Fe₃O₄-PEI NPs was

assessed by X-ray powder diffraction, XRD (XRD-6000, Shimadzu). Ultraviolet visible (UV–Vis) spectra measurements were done using (Jasco-530 spectrophotometer) at the range of 400–800 nm. Hydrodynamic size distribution (DLS) and zeta potential analysis were done by Zetasizer (ZEN3600, Malvern) in deionized water at room temperature. Size and morphology of the dried samples were evaluated by field emission scanning electron microscopy, FE-SEM (MIRA III, Tescan) and transmission electron microscopy, TEM (CM30, Philips). Elemental analysis of the samples was carried out by energy dispersive spectrometry, EDX (MIRA III, Tescan), MAP (MIRA III, Tescan), and inductively coupled plasma mass spectrometry, ICP-MS (7900, Agilent). Amount of PEI coating in Fe₃O₄-PEI NPs was determined via Thermogravimetric analysis, TGA (METTLER TOLEDO). Magnetic property of the samples was evaluated by vibrating sample magnetometer, VSM (Meghnatis Kavir Kashan Co., Kashan, Iran) with a maximum magnetic field of 10 kOe at 25 °C.

3 Results and Discussion

3.1 FTIR Analysis

Figure S1a (supporting information) shows the FTIR spectrum of Fe₃O₄ NPs. The observed peaks at 576, 1615, and 3395 cm⁻¹ were respectively related to vibration of Fe–O bond, the bending vibration of –OH bond, and vibration of –OH, which could confirm the formation of Fe₃O₄ NPs covered with hydroxyl groups [27]. In FTIR spectrum of Fe₃O₄-PEI NPs (Fig. S1b, supporting information), the observed peak at 582 cm⁻¹ was related to Fe–O bond; also, the peaks at 2854 and 2923 cm⁻¹ were ascribed to C–H bond, and the peak at 3400 cm⁻¹ was attributed to N–H bond. The presence of the peaks of C–H and N–H bonds along with the peak of Fe–O bond could confirm the electrostatic binding of PEI to the surface of Fe₃O₄ NPs [28]. It should be noted that the peak of N–H bond has had an overlap with the peak related to –OH bond. Fig. S1c (supporting information) shows the FTIR spectrum of Fe₃O₄-PEI-CUR NPs in

which in addition to the characteristic peaks of Fe₃O₄ NPs at 576 cm⁻¹ and PEI-related peaks at 2800 and 2900 cm⁻¹, the appeared characteristic peaks of CUR at 1600 cm⁻¹ (C=C bond) and 1627 cm⁻¹ (C=O bond) could confirm the successful loading of CUR on Fe₃O₄-PEI NPs [29, 30]. Other observed peaks were in accordance with the standard FTIR spectrum of CUR.

3.2 XRD Analysis

Figure 1 shows the X-ray diffraction (XRD) pattern of Fe₃O₄-PEI NPs. The Fe₃O₄ characteristic peaks were at 2θ of 30.6, 35.9, 43.3, 57.4, and 63.2. A slight expansion of the peaks, while there was no noticeable displacement, could indicate the formation of Fe₃O₄ NPs' crystals with PEI coating. Also, the appeared peaks for Fe₃O₄-PEI NPs were in agreement with standard peaks of Fe₃O₄ NPs (JCPDS card 72-2303) which could indicate no change in crystalline structure of Fe₃O₄ after PEI coating [31].

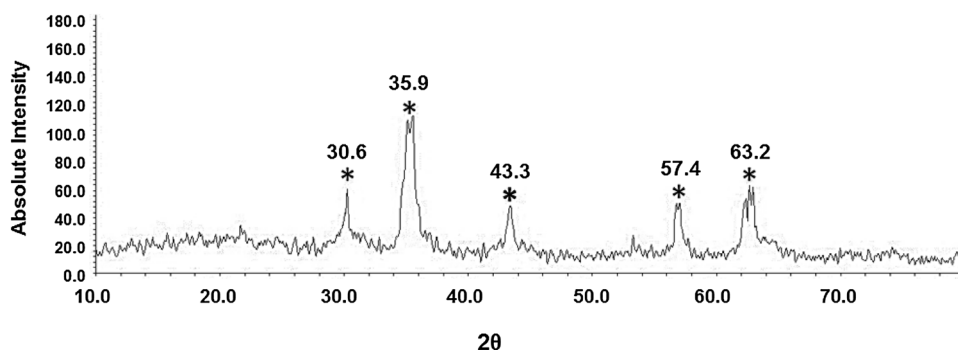
3.3 DLS Analysis

Figure S2 (supporting information) illustrates the Dynamic Light Scattering (DLS) diagram. In this analysis, the approximate size of the fabricated NPs was primarily determined, so that the size of Fe₃O₄ NPs was 30 nm, the size of Fe₃O₄-PEI NPs was 60 nm, and the size of Fe₃O₄-PEI-CUR NPs was about 60 nm.

3.4 Zeta Potential Analysis

Figure S3 (supporting information) shows the diagram of zeta potential analysis for Fe₃O₄, Fe₃O₄-PEI, and Fe₃O₄-PEI-CUR NPs. This analysis provides information about the surface charge of NPs. As can be seen, the zeta potential for Fe₃O₄ NPs was –4 (mv) which could be related to the negative charge of hydroxyl groups on their surface. Also, the zeta potential for Fe₃O₄-PEI NPs was +25 (mv) which could be attributed to the positive charge presented by amine groups of PEI. Positive surface charge of the NPs after their coating with PEI could also

Fig. 1 XRD pattern of Fe₃O₄-PEI NPs. Fe₃O₄ characteristic peaks are indicated by (*)

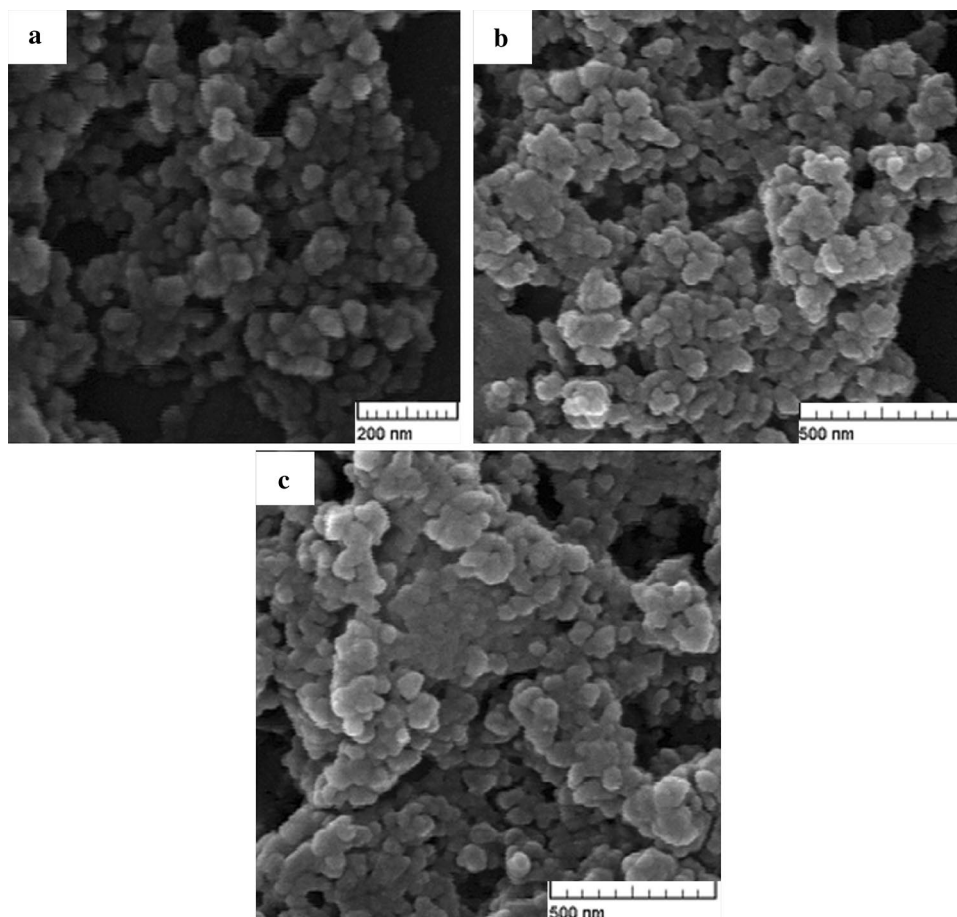


confirm the formation of Fe_3O_4 -PEI NPs. Moreover, the surface charge of Fe_3O_4 -PEI-CUR NPs was about -2.7 (mv) which, as compared to positive charge of Fe_3O_4 -PEI NPs, could indicate the presence of CUR on the surface of these NPs owing to the negative charge associated with hydroxyl groups of CUR. This could be another sign for successful loading of CUR on Fe_3O_4 -PEI NPs.

3.5 SEM Analysis

Figure 2a, b, c illustrate the scanning electron microscopy (SEM) images of the fabricated NPs. SEM, as a supplementary analysis, provides good information about the shape and size of NPs. The size of the Fe_3O_4 , Fe_3O_4 -PEI, and Fe_3O_4 -PEI-CUR NPs was about 25, 55 and 55 nm, respectively, and their shape was almost spherical. According to a report by Gref et al. [32], size of NPs should be below 100 nm in order to prevent them from being removed by the RES and hence to increase their half-life in the bloodstream. Therefore, the size of the fabricated NPs was determined suitable for clinical applications.

Fig. 2 SEM images of Fe_3O_4 (a), Fe_3O_4 -PEI (b), and Fe_3O_4 -PEI-CUR (c) NPs



3.6 EDX Analysis

Figure S4 (supporting information) shows the result of (EDX) analysis for determining the distribution of elements for Fe_3O_4 -PEI-CUR NPs. The obtained result confirmed the presence of the key elements in the Fe_3O_4 -PEI-CUR NPs structure, i.e., C, N, O and Fe, in the regions of 0.25, 0.4, 0.5, and (0.7, 6.3) (keV), respectively.

3.7 MAP Analysis

MAP analysis shows the distribution of elements visually as a map. Fig. S5 (supporting information) depicts the map of distribution of Fe_3O_4 -PEI-CUR NPs' key elements (i.e., C, N, O, and Fe) which was in accordance with the result of EDX analysis.

3.8 TEM Analysis

Figure 3 shows the transmitted electron microscope (TEM) image of Fe_3O_4 -PEI NPs. According to the image, the size of the NPs was about 50 nm, and their shape was almost spherical.

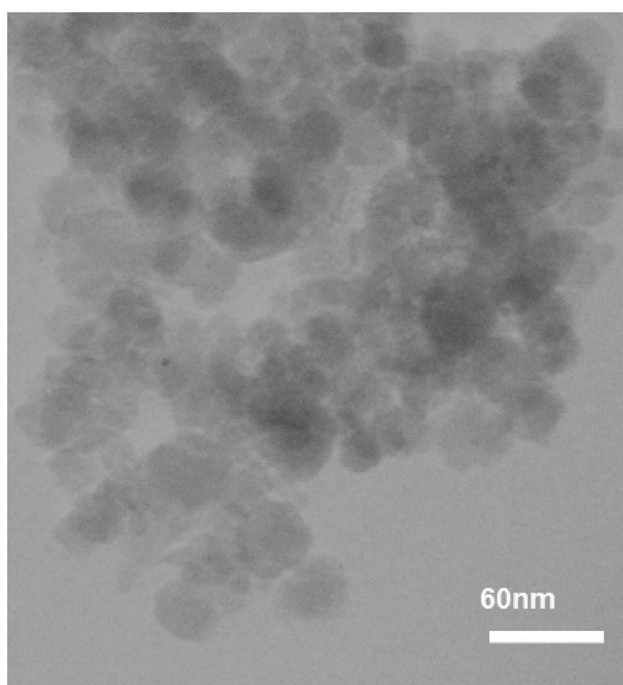
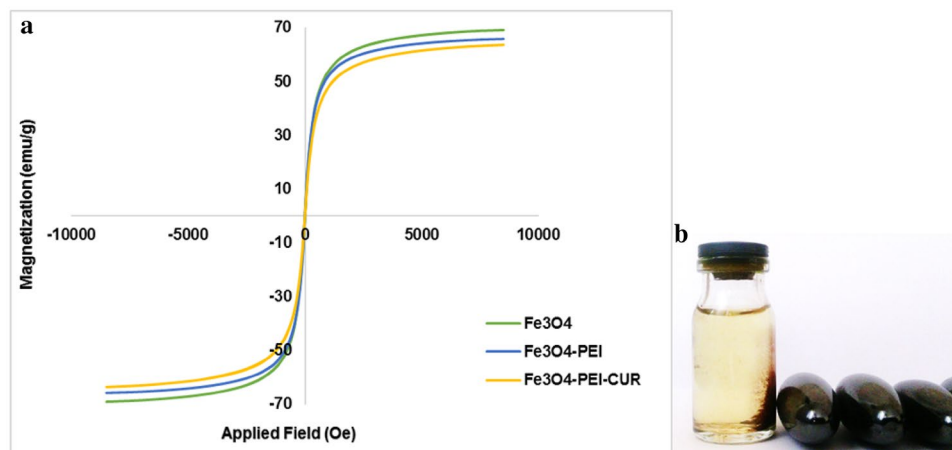


Fig. 3 TEM image of Fe_3O_4 -PEI NPs

3.9 TGA Analysis

In order to determine the PEI weight percentage in Fe_3O_4 -PEI NPs, thermogravimetric analysis (TGA) was applied. According to thermogram of Fe_3O_4 -PEI NPs (Fig. S6, supporting information), weight loss was observed in two steps; the first stage of weight loss was about 1.45% at the range of 30–130 °C which could be related to the evaporation of trapped water in the structure of the NPs. The second weight loss was about 10% at the range of 130–420 °C which could be attributed to the degradation of the PEI layer on the surface of the NPs and consequently to the weight percentage of PEI.

Fig. 4 Results of the VSM analysis for Fe_3O_4 , Fe_3O_4 -PEI, and Fe_3O_4 -PEI-CUR NPs (a) and response of Fe_3O_4 -PEI-CUR NPs to external magnetic field (b)



3.10 VSM Analysis

Figure 4a illustrates the results of the VSM analysis for Fe_3O_4 , Fe_3O_4 -PEI, and Fe_3O_4 -PEI-CUR NPs. VSM shows the magnetic properties of the NPs in (emu/g) unit. As seen, the magnetic properties of Fe_3O_4 , Fe_3O_4 -PEI, and Fe_3O_4 -PEI-CUR NPs were obtained 69, 65, and 63 (emu/g), respectively. A decrease of about 4 units in the magnetic property of the Fe_3O_4 NPs after the addition of PEI coating and also a decrease of about 2 units in the magnetic property of Fe_3O_4 -PEI NPs after the addition of CUR were ascribed to the non-magnetic property of PEI and CUR. However, the decrease in the magnetic property of these NPs was not significant enough to affect their response to an external magnetic field. As shown in Fig. 4b, dispersed Fe_3O_4 -PEI-CUR NPs were separated from water and directed toward the magnet as exposed to an external magnetic field. The result of this analysis could indicate that the fabricated NPs were suitable for use as a MRI contrast agent.

3.11 CUR Loading on Fe_3O_4 -PEI NPs (Fe_3O_4 -PEI-CUR NPs)

In order to determine the amount of the CUR loaded on Fe_3O_4 -PEI NPs, the calibration curve of CUR was first plotted in a solution of water and acetone with a volume ratio of 10:1. For this purpose, different concentrations of this solution were prepared, and absorbance of each of them at 420 nm was recorded via UV–Vis. Fig. S7 (supporting information) illustrates the calibration curve associated with the loading process. By using the formula derived from the calibration curve and also the relationships indicated in Sect. 2.2.3, the content and the percentage of loaded CUR on Fe_3O_4 -PEI NPs in different weight ratios of CUR to the NPs (i.e., 1:1, 2:1 and 3:1) were determined as follows (Table 1):

As seen, with a twofold increase in the weight ratio of CUR to Fe_3O_4 -PEI NPs, the CUR content increased about

Table 1 Results of CUR loading at different CUR to Fe₃O₄-PEI NPs weight ratios

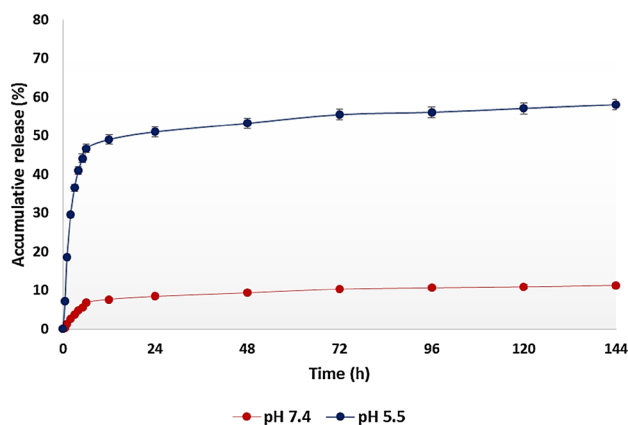
CUR to Fe ₃ O ₄ -PEI NPs weight ratios	Loading content of CUR (LC) (mg of CUR/1 mg of Fe ₃ O ₄ -PEI NPs)	Percentage of loaded CUR on Fe ₃ O ₄ -PEI NPs (PL) (%)
1:1	0.41	30
2:1	0.63	38
3:1	0.6	37.5

0.22 (mg/mg of Fe₃O₄-PEI NPs). In addition, 8% increase in the percentage of loaded CUR was observed. But with a threefold increase in the weight ratio of CUR to Fe₃O₄-PEI NPs, no considerable increase in the amount of loaded CUR was observed. In this case, the weight content and the percentage of loaded CUR were as same as the weight ratio of 2:1 with an approximation of less than 5%. Hence, it could be concluded that more than twofold increase in the weight ratio of CUR to Fe₃O₄-PEI NPs did not lead to considerable increase in the amount of loaded CUR, so the optimum ratio was 2:1.

3.12 Evaluation of CUR Release Profile Form Fe₃O₄-PEI-CUR NPs

In order to evaluate the profile of CUR release from Fe₃O₄-PEI-CUR NPs, the calibration curves associated with CUR release in PBS solution (0.1% w/v of Tween-80 at pH 5.5 and 7.4) were plotted first (Fig. S8a&S8b, supporting information). The process of plotting calibration curves for CUR release was similar to that of CUR loading.

The profile of CUR release from Fe₃O₄-PEI-CUR NPs was achieved using the above calibration curves at pH 5.5 and 7.4 (Fig. 5). As shown, CUR release from Fe₃O₄-PEI-CUR NPs at pH 5.5, which represented the intra tumor environment [33], was much faster and more than that in pH 7.4, which represented the blood plasma environment. Thus, in the first 6 h at pH 5.5, CUR release was about 46%, while it was about 7% at pH 7.4. Also, in the first 24 h at pH 5.5, there was a burst release of CUR about 51%, while at pH 7.4, the amount of CUR released in the same time was merely about 9%. In addition, it was observed that the raising release rate of CUR stopped after 72 h at both pH 5.5 and 7.4, so that after approximately 144 h (6 days) it reached a constant level of 58% at pH 5.5 and 11% at pH 7.4. The results indicated that the release of CUR from Fe₃O₄-PEI-CUR NPs was pH-sensitive which could reduce its side effects for healthy tissues because CUR release around healthy tissues (pH 7.4) could be apparently much lower than that in intra tumor environment (pH 5.5). Fig. S9a&S9b (supporting information) show the photographs of supernatant solutions for the first 6 h of CUR release from

**Fig. 5** CUR release profile from Fe₃O₄-PEI-CUR NPs at pH 5.5 and 7.4

Fe₃O₄-PEI-CUR NPs at pH 5.5 and 7.4. As it was visually evident, the concentration of solutions at pH 5.5 was clearly higher than that at pH 7.4.

3.13 HPLC Analysis

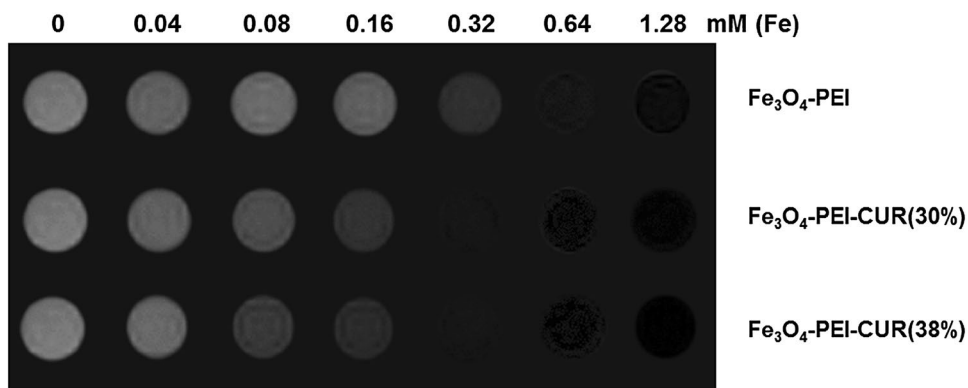
According to the obtained results (Fig. S10a&S10b, supporting information), the peak of the CUR at 420 nm gradually formed after about 2 min and was completed in the interval of 2.3 up to 2.5 min. This results further confirmed the presence of CUR in supernatant solutions of release process.

3.14 In Vitro MRI

The magnetic properties of magnetic NPs, as contrast agents, are used to differentiate between normal and affected tissues and, consequently, to investigate affected tissue conditions appropriately. In this project, the effect of CUR presence in the structure of Fe₃O₄-PEI NPs was investigated in increasing the contrast in MRI images. For this purpose, the applicability of CUR loaded Fe₃O₄-PEI NPs as negative contrast agents of MRI with two different composition percentages of: (1) CUR 30% (Fe₃O₄-PEI-CUR (30%)) and (2) CUR 38% (Fe₃O₄-PEI-CUR (38%)) was studied through determining the T₂ values of protons in their aqueous solutions. Moreover, the obtained images and quantitative results were assessed at diverse concentrations of these three samples including Fe₃O₄-PEI, Fe₃O₄-PEI-CUR (30%), and Fe₃O₄-PEI-CUR (38%) NPs.

As shown in Fig. 6, it was observed visually and qualitatively that all three samples reduced T₂-weighted magnetic resonance (MR) signal intensity as compared to control sample (Fe = 0 M, PBS pH 7.4). In addition, the contrast generated by Fe₃O₄-PEI-CUR (30%) NPs was more than that of Fe₃O₄-PEI NPs, and the contrast caused by Fe₃O₄-PEI-CUR (38%) NPs was slightly more than that of Fe₃O₄-PEI-CUR

Fig. 6 In vitro T_2 -weighted MRI images of Fe_3O_4 -PEI, Fe_3O_4 -PEI-CUR (30%), and Fe_3O_4 -PEI-CUR (38%) NPs



(30%) NPs; in fact, it could be said that their images were almost similar.

Along with visual or qualitative data, in vitro MRI also contains some useful quantitative data to review. The value of r_2 relaxation rate (1/mM sec) is an important numerical datum that indicates the material's ability to cause negative contrast. Figure 7a, b, c show the graphs of $1/T_2$ values versus the concentrations of Fe for Fe_3O_4 -PEI, Fe_3O_4 -PEI-CUR (30%), and Fe_3O_4 -PEI-CUR (38%) NPs, so that the gradients show the derived r_2 relaxation rate values. As can be seen, the r_2 values for Fe_3O_4 -PEI, Fe_3O_4 -PEI-CUR (30%), and Fe_3O_4 -PEI-CUR (38%) NPs were 78.278, 93.854, and 95.685 (1/mM.sec), respectively. Thus, the r_2 of the CUR loaded NPs (i.e., Fe_3O_4 -PEI-CUR

(30%)) increased by about 20% as compared to Fe_3O_4 -PEI NPs. In addition, with the CUR content increase of about 8% in Fe_3O_4 -PEI-CUR (38%) NPs, r_2 raised only about 2% as compared to that of Fe_3O_4 -PEI-CUR (30%) NPs. The results indicated that there was a significant difference in the ability of CUR-free and CUR-containing NPs to cause negative contrast which was in accordance with the results of previously reported studies [21]; however, an 8% increase in CUR content of CUR-containing NPs did not produce a significant difference in r_2 values of Fe_3O_4 -PEI-CUR (30%) and Fe_3O_4 -PEI-CUR (38%) NPs. This might be due to the fact that the color content of CUR only could increase the r_2 up to a certain extent at a certain concentration that finally reached a steady state.

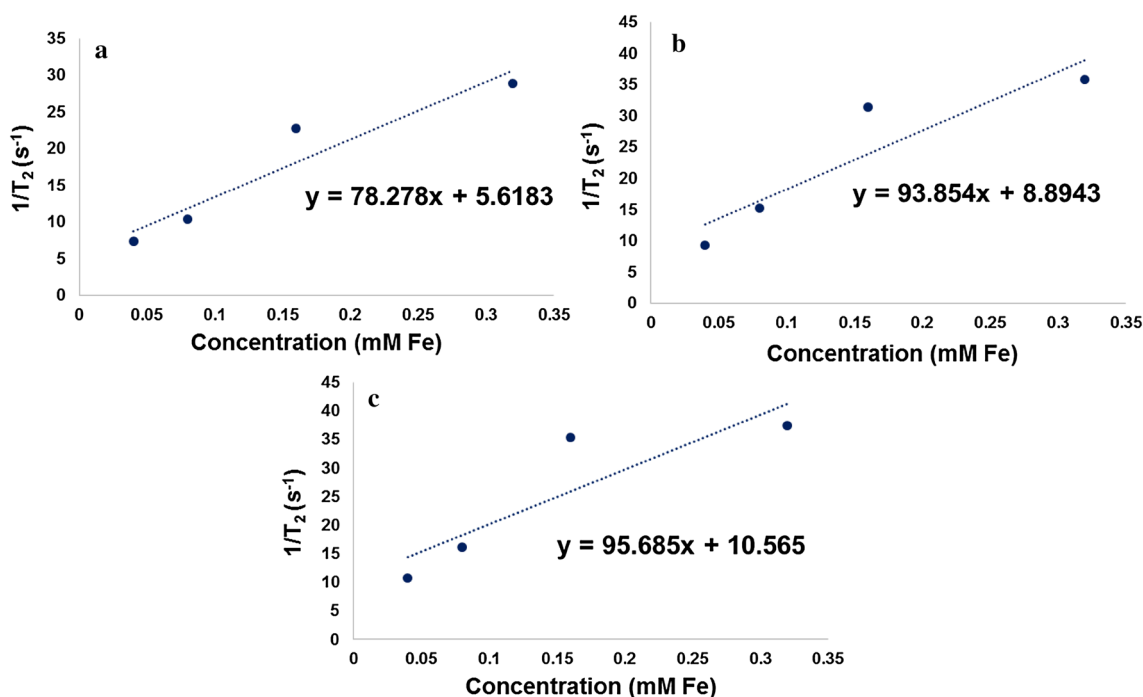


Fig. 7 T_2 relaxation rates ($1/T_2$) plotted against Fe concentrations for Fe_3O_4 -PEI (a), Fe_3O_4 -PEI-CUR (b) (30%), and Fe_3O_4 -PEI-CUR (38%) (c) NPs

Other advantageous quantitative data from in vitro MRI are the curves of the signal intensity changes against the TE values. Figure 8a, b, c show the curves of signal intensity alterations against TE values for Fe₃O₄-PEI, Fe₃O₄-PEI-CUR (30%), and Fe₃O₄-PEI-CUR (38%) NPs at different Fe concentrations. As seen, for all three samples, signal intensity decreased with increasing Fe concentration which could indicate the ability of the fabricated NPs to create negative contrast and the impact of Fe concentration on creating more contrast relative to control. The results were in agreement with the results of Fig. 6. In addition, Fe₃O₄-PEI-CUR (30%) NPs, at different concentrations as compared to Fe₃O₄-PEI NPs, reduced the signal intensity more by about 60%, which was consistent with the results observed in Fig. 6 and also the determined values of r_2 . It is worth noting that there is no linear relationship between r_2 and signal intensity variations. Besides, Fe₃O₄-PEI-CUR NPs (38%) reduced the signal intensity by about 15% more than Fe₃O₄-PEI-CUR (30%) NPs at diverse concentrations. These results were also in relative accordance with the results obtained from Fig. 6 and the calculated r_2 values.

As shown, the results gained from signal intensity alteration curves against TE values indicated the effect of the presence of CUR on increasing the negative contrast in MRI images as compared to CUR-free Fe₃O₄-PEI NPs. Nonetheless, an increase of about 8% in the amount of CUR in Fe₃O₄-PEI-CUR (38%) NPs only resulted in a 15% reduction in signal intensity relative to Fe₃O₄-PEI-CUR NPs

(30%) NPs, which was inconsiderable in comparison with the 60% difference in signal intensity reduction between Fe₃O₄-PEI-CUR (30%) and Fe₃O₄-PEI NPs.

Iron oxide based superparamagnetic NPs also have the ability to reduce T₂*-weighted MR signal intensity [26]. T₂* relaxation time is considered as effective or observed T₂ in which signal intensity reduces faster than T₂. T₂* is caused by heterogeneity in the main magnetic field, and its application is in imaging of heterogeneous tissues (e.g., for the detection of small internal hemorrhages) [34]. As shown in Fig. 9, T₂*-weighted MRI images were brighter than T₂-weighted ones. Similarly to the results of T₂-weighted images (Fig. 6), in T₂*-weighted images, the contrast caused by Fe₃O₄-PEI-CUR (30%) NPs was more than the contrast produced by Fe₃O₄-PEI NPs, which could be due to the presence of CUR as a color containing substance. Moreover, the contrast created by Fe₃O₄-PEI-CUR (38%) NPs was slightly more than that of Fe₃O₄-PEI-CUR (30%) NPs, as it can be said that their images were nearly comparable.

4 Conclusion

Based on the achieved results, the structure of the fabricated Fe₃O₄-PEI-CUR NPs was validated according to the initial hypothesis (i.e., NPs of about 50 nm in diameter with acceptable magnetic properties). Also, CUR to Fe₃O₄-PEI NPs weight ratio of 2:1 was determined as an

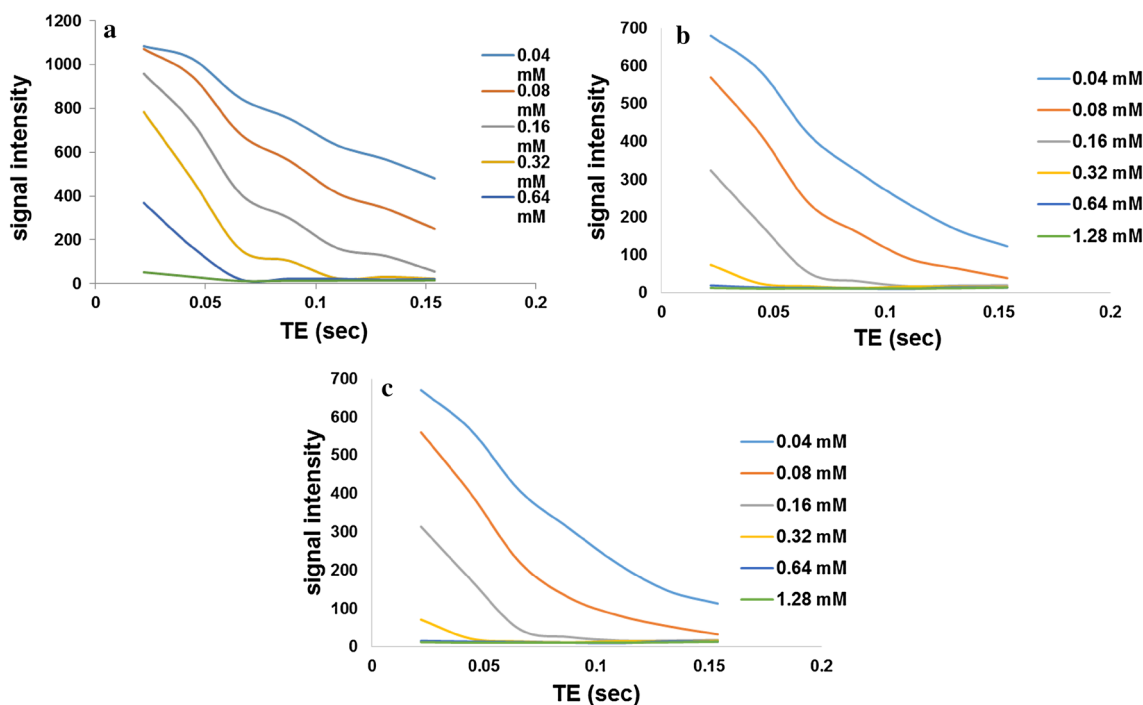
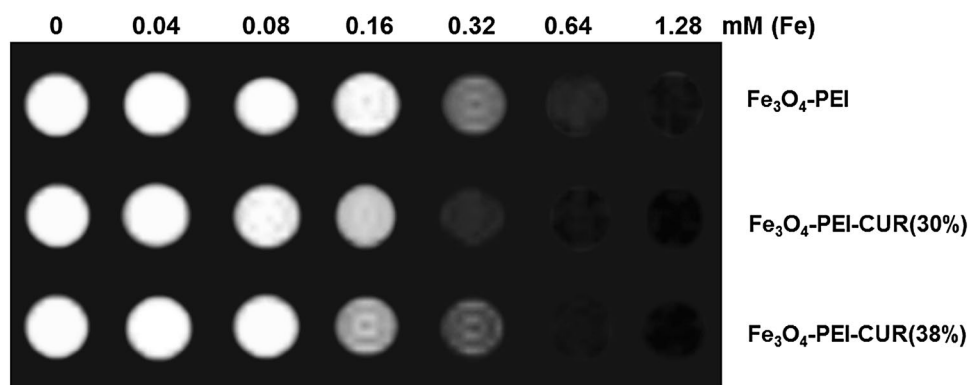


Fig. 8 Signal intensity alteration curves for Fe₃O₄-PEI (a), Fe₃O₄-PEI-CUR (b) (30%), and Fe₃O₄-PEI-CUR (38%) (c) NPs

Fig. 9 In vitro T_2^* -weighted MRI images of Fe_3O_4 -PEI, Fe_3O_4 -PEI-CUR (30%), and Fe_3O_4 -PEI-CUR (38%) NPs



optimal ratio resulting in an 8% increase in the amount of loaded CUR as compared to the ratio of 1:1. In addition, CUR release from Fe_3O_4 -PEI-CUR NPs was evaluated at pH of 5.5 and 7.4 which revealed that the mechanism of release was pH-sensitive. The visual and numerical data of in vitro MRI including the r_2 relaxation rate values for Fe_3O_4 -PEI, Fe_3O_4 -PEI-CUR (30%), and Fe_3O_4 -PEI-CUR (38%) NPs, which were determined 78.278, 93.854, and 95.685 (1/mM sec), respectively, and signal intensity alteration curves all indicated an enhancement in negative contrast in the presence of CUR. Although there was a 20% difference between r_2 values of Fe_3O_4 -PEI and Fe_3O_4 -PEI-CUR (30%) NPs, it was shown that an 8% increase in the amount of CUR in Fe_3O_4 -PEI-CUR (38%) NPs only resulted in about 2% increase of r_2 value, which was not significant and indicated that CUR content more than a certain amount could not increase r_2 value considerably.

Acknowledgements This research was granted by AJA University of medical sciences, Tehran, Iran.

Compliance with Ethical Standards

Conflict of interest The authors declare that they have no conflict of interest.

References

- W. Hollingworth et al., *Clin. Radiol.* **55**, 825–831 (2000)
- Z.R. Stephen, F.M. Kievit, M. Zhang, *Mater. Today* **14**, 330–338 (2011)
- M. De, S.S. Chou, H.M. Joshi, V.P. Dravid, *Adv. Drug Deliv. Rev.* **63**, 1282–1299 (2011)
- D. Niu et al., *ACS Appl. Mater. Interfaces* **5**, 9942–9948 (2013)
- H. Liu et al. *Proc. Natl. Acad. Sci. USA* **107**, 15205–15210 (2010)
- B. Chertok, A.E. David, V.C. Yang, *Biomaterials* **31**, 6317–6324 (2010)
- A.C. Silva et al., *Int. J. Nanomed.* **6**, 591–603 (2011)
- K. Maier-Hauff et al., *J. Neurooncol.* **103**, 317–324 (2011)
- C. Sun et al., *Nanomedicine* **3**, 495–505 (2008)
- B. Tomanek et al., *Neuro Oncol.* **14**, 53–63 (2012)
- S.D. Kong et al., *J. Control Release* **164**, 49–57 (2012)
- P.A. Voltairas, D.I. Fotiadis, L.K. Michalis, *J. Biomech.* **35**, 813–821 (2002)
- O. Boussif et al., *Proc. Natl. Acad. Sci.* **92**, 7297–7301 (1995)
- J. Li et al., *J. Drug Target* **19**, 814–820 (2011)
- C.Y. Tay, N. Menon, D.T. Leong, L.P. Tan, *J. Inorg. Organomet. Polym. Mater.* **25**, 301–311 (2015)
- R. Wilken, M.S. Veena, M.B. Wang, E.S. Srivatsan, *Mol. Cancer* **10**, 12 (2011)
- M.M. Yallapu, M. Jaggi, S.C. Chauhan, *Coll. Surf. B* **79**, 113–125 (2010)
- T.K. Jain, M.a. Morales, S.K. Sahoo, D.L. Leslie-Pelecky, V. Labhasetwar, *Mol. Pharm.* **2**, 194–205 (2005)
- S.S. Banerjee, D.-H. Chen, *Nanotechnology* **19**, 265602 (2008)
- H. Zhu et al., *Biomaterials* **34**, 2296–2306 (2013)
- M.M. Yallapu et al., *Int. J. Nanomed.* **7**, 1761–1779 (2012)
- L. Wang et al., *Int. J. Cancer* **136**, 107–116 (2015)
- F. Dilnawaz, A. Singh, S.K. Sahoo, *Acta Biomater.* **8**, 704–719 (2012)
- M. Song et al., *Coll. Surf. A* **408**, 114–121 (2012)
- D.-F. Liu et al., *Nanoscale* **6**, 15161–15167 (2014)
- M.A. Shevtsov et al., *Int. J. Nanomed.* **9**, 273–287 (2014)
- A.K. Bordbar et al., *Biotechnol. Res. Int.* **2014**, 705068 (2014)
- X. Yang, J.C. Kim, *Int. J. Biol. Macromol.* **48**, 661–666 (2011)
- T.M. Kolev, E.A. Velcheva, B.A. Stamboliyska, M. Spittler, *Int. J. Quantum Chem.* **102**, 1069–1079 (2005)
- V.T. Bich et al., *Springer Proc. Phys.* **127**, 271–278 (2009)
- C. Schweiger, C. Pietzonka, J. Heverhagen, T. Kissel, *Int. J. Pharm.* **408**, 130–137 (2011)
- R. Gref et al., *Science* **263**, 1600–1603 (1994)
- Y. Xiao et al., *Biomaterials* **33**, 3071–3082 (2012)
- G.B. Chavhan, P.S. Babyn, B. Thomas, M.M. Shroff, E.M. Haacke, *Radiographics* **29**, 1433–1449 (2009)